Journal of Reproduction and Development, Vol. 61, No 5, 2015

—Original Article—

Malfunction of spermatogenesis in experimental ischemic mice

Futoshi YAZAMA[1)], Haruki SATO[1)] and Tomoko SONODA[2)]

[1)]*Laboratory of Cell Biology and Morphology, Department of Life Science, Prefectural University of Hiroshima, Hiroshima 727-0023, Japan*

[2)]*Laboratory of Molecular Physiology, Department of Molecular Biodefence Research, Yokohama City University School of Medicine, Yokohama 236-0004, Japan*

Abstract. An experimental ischemia (EI)-induced mouse model was used to analyze pathological and biochemical alterations in testes. Initial morphological changes were observed in Sertoli cells of EI testes at the light microscopic level. Examination of the ultrastructure using transmission electron microscopy confirmed that Sertoli cells were partially detached from the basement membrane of the seminiferous epithelium and that the cell membranes of adjacent Sertoli cells were not joined. The functional integrity of the blood-testis barrier (BTB) was assessed using the lanthanum tracer technique. Lanthanum had penetrated into the spaces between adjacent Sertoli cells in the adluminal compartment up to the lumen of the seminiferous epithelium in EI testes. Proteome analysis showed that the expression of heat shock protein (HSP) 70 was significantly upregulated in EI testes. Western blot analysis confirmed that the expression of HSP70 increased in a time-dependent manner after the EI procedure. HSP70 immunostaining was observed in spermatocytes and in round and elongated spermatids in EI testes. Our results suggest that a change in the junctions between adjacent Sertoli cells on the basal compartment is involved in the BTB disruption in EI testes. Therefore, male infertility caused by the BTB disruption could be associated with heat stress induced by ischemia.

Key words: Blood-testis barrier (BTB), Heat shock protein (HSP) 70, Ischemia, Mouse, Testis

(**J. Reprod. Dev. 61:** 399–406, 2015)

Infertility affects an estimated 15% of couples seeking to have children, and in approximately half of these cases, the defect can be attributed to the man [1–3]. Several studies have reported an association of regional declines in sperm counts and increases in abnormal spermatogenesis with male reproductive disorders [4, 5]. Approximately 40% of male infertility is caused by known etiologies such as undescended testes, varicocele or hypogonadism; however, the etiology and pathogenesis of these disorders are still not fully understood in a significant percentage of cases, and these cases are referred to as idiopathic infertility [6, 7].

In most mammals, the testes are kept at about 5 C below the body temperature, and this is the reason for their descent into the scrotum. Cooling of testes depends, in part, on perspiration and evaporative heat loss from the surface of the scrotum. In addition to the scrotum, a second thermoregulatory system is located in the spermatic cord; this uses a countercurrent heat exchange between incoming arterial blood and outgoing venous blood [8].

Here, we explored the interplay between spermatogenesis and heat stress induced by ischemia and the pathogenic mechanism underlying male infertility by morphological and biochemical analyses of mice testes in an experimental ischemia (EI)-induced mouse model.

Received: March 3, 2015
Accepted: May 12, 2015
Published online in J-STAGE: June 9, 2015

Correspondence: F Yazama (e-mail: fyzma@pu-hiroshima.ac.jp)

Materials and Methods

Surgery for EI induction

ICR male mice (35 days old, CLEA Japan) were anesthetized with an intraperitoneal injection of pentobarbital (5 mg/kg). A scrotum incision was made. Careful dissection of the area between the head of the epididymis and the testis was performed. The left testicular artery and vein were identified and clamped. The right testicular artery and vein between the head of the epididymis and the testis were also identified by scrotum incision (sham operation). The experiments were approved by the Ethics Committee for Animal Experiments of the Prefectural University of Hiroshima, Shobara campus, Japan (ID: 12SA014).

Morphological analysis

Fully anesthetized mice were perfused (after removal of the clamp) with either a periodate-lysine-paraformaldehyde (PLP) fixative [9] or 2% paraformaldehyde (PFA) and 2.5% glutaraldehyde (GA) in 0.1 M phosphate buffer (PB; pH 7.2) via the left ventricle at room temperature (RT), and then the testes were immersed in the same fixative for 2 h at RT. Testes were prepared at 0, 60, 120, 180, 240 and 300 min after the EI procedure (10 mice used for each time point), and the right testes (sham operation) were used as controls.

The PLP-fixed testes were dehydrated in an ethanol series and embedded in paraffin. Paraffin sections were cut into 5-μm slices. For immunocytochemistry, paraffin sections were blocked with 50% calf serum in 0.1 M PB (pH 7.2) for 1 h at RT and incubated for 1 h at RT with the heat shock protein (HSP) 70 polyclonal antibody (diluted 1:200 in blocking solution, ADI-SPA-812; Enzo Life Sciences,

Farmingdale, NY, USA). They were then labeled with an HRP-conjugated secondary antibody (diluted 1:1,000 in blocking solution, sc-3837; Santa Cruz Biotechnology, Dallas, TX, USA). Peroxidase activity was detected after the addition of diaminobenzidine (D4293, SIGMAFAST 3,3'-Diaminobenzidine tablets; Sigma-Aldrich, St. Louis, MO, USA). Slides were counterstained with hematoxylin. Immunoperoxidase localization of HSP70 was recorded using a ScopePad-500 (Gellex International, Tokyo, Japan) attached to a light microscope (ECLIPSE E400; Nikon, Tokyo, Japan). All images were processed using the Adobe Photoshop CS5 software (Adobe, San Jose, CA, USA) to reflect the original image as closely as possible.

For conventional transmission electron microscopy (TEM), small pieces of fixed testicular tissue were postfixed with 1% osmium in 0.1 M PB (pH 7.2) at 4 C for 90 min, dehydrated using an ethanol series and embedded in Epon 812 (TAAB Laboratories, Berkshire, England). Semithin sections were stained with 1% toluidine blue (TB) dye and examined under a light microscope. Ultrathin sections were double stained with uranyl acetate and lead nitrate and examined using a JEM-1200EX II TEM (JEOL, Tokyo, Japan) operated at 80 kV. To obtain an intercellular tracer, 4% aqueous lanthanum nitrate was mixed with an equal volume of 4% GA in 0.2 M cacodylate buffer (pH 7.2) and used to fix the testis tissue. Tissues were postfixed in 0.1 M cacodylate-buffered osmium tetroxide with 2% lanthanum nitrate. After dehydration and embedding, the sections were examined without staining.

Biochemical analysis

The testes (right testes at 0 min and EI testes after 180 min) were removed surgically from fully anesthetized mice and decapsulated, and the main testicular blood vessel was excised. The testes (0.1 g) were homogenized with 1,000 µl of lysis buffer (8 M urea in distilled water containing 2% IGEPAL CA-630, 2% ampholine pH 4.0–8.0, 5% β-mercaptoethanol and 5% polyvinylpyrrolidone). The insoluble materials were removed by centrifugation (15,000 rpm for 30 min at 4 C). The supernatant (200 µl) was subjected to isoelectric focusing (IEF). In brief, two-dimensional (2D) electrophoresis was performed as described previously [10], but it was modified to improve the resolution [11]. The first dimension, IEF, was run in a stepwise manner: 200 V for the first 0.5 h, 300 V for 0.5 h, 400 V for 18 h and finally 800 V for 1 h. After the second dimension, sodium dodecyl sulfate polyacrylamide gel electrophoresis (SDS-PAGE), protein spots were detected using Coomassie Brilliant Blue (CBB) R-250. For protein identification, the protein spots were excised and digested with V8 protease according to the Cleveland method [12]. The digested peptides were transferred to a polyvinylidene difluoride (PVDF) membrane and stained with CBB. The CBB-stained peptides were excised directly from the PVDF membrane, and the internal N-terminal sequence was obtained on a peptide sequencer (PPSQ-21; Shimadzu, Kyoto, Japan). Peptide identification was performed using FASTA search (http://www.genome.jp/tools/fasta/).

For SDS-PAGE, six types of testis samples (0, 60, 120, 180, 240 and 300 min after EI) were used. The testes (0.1 g) were homogenized with 2,000 µl of sample buffer [0.5 M Tris-HCl (pH 6.8), 2% SDS, 5% β-mercaptoethanol and 10% glycerol], and the insoluble material was removed by centrifugation (15,000 rpm for 30 min at 4 C). The supernatant (5 µl) was electrophoresed on 12% polyacrylamide slab gels using the method of Hirano and W-Liebold [13]. The protein bands were stained with CBB.

For Western blotting, the electrophoresed proteins were transferred to nitrocellulose (NC) membranes for 8 h at 4 C at the constant voltage of 10 V. The NC membranes were stained with Ponceau S to visualize the positions of the major bands and to determine the efficiency of the transfer. The NC membranes were then cut into strips, blocked with 3% nonfat dry milk in TBS [150 mM NaCl, 10 mM Tris-HCl (pH 7.4)] for 1 h at RT and incubated for 1 h at RT with the anti-HSP70 antibody (diluted 1:500 in blocking solution). The strips were rinsed and incubated for 1 h at RT with anti-rabbit IgG conjugated with peroxidase (final dilution 1:1,000, MBL, Nagoya, Japan). Detection of the antibody was performed using a peroxidase substrate (TrueBlue; KPL, Gaithersburg, MD, USA).

Statistical analysis

The images of Western blotting were processed using the public-domain NIH Image program (http://rsb.info.nih.gov/nih-image/) and Adobe Photoshop CS5 software. Data were analyzed using the Student's *t* test. A P-value of < 0.05 was considered statistically significant.

Results

Light microscopy

Figure 1 shows semithin sections of the control (A), 240 min after EI (B; EI-240) and EI-300 testes (C). Normal spermatogenesis was observed in the control testes (Fig. 1A). In EI-240 testes, the seminiferous epithelium was partially detached from the testicular lamina propria (Fig. 1B). By contrast to the control testes (Fig. 1A), degenerating seminiferous tubules were observed in EI-300 testes (Fig. 1C, asterisks). At the light microscopic (LM) level, the general morphology of the seminiferous tubules in EI-180 testes (Fig. 2B) was similar to that of the control testes (Fig. 2A). However, there were some parts densely stained with TB dye in the seminiferous epithelium in EI-180 testes (Fig. 2B, white arrows). There was no evidence of spermatogenesis in EI-300 seminiferous tubule (Fig. 2C, asterisk).

Electron microscopy

TEM examination of the ultrastructures confirmed that in the EI-240 testes, the regions densely stained with TB dye at the LM level (Fig. 2B, white arrows) were the Sertoli cells in the seminiferous epithelium (Fig. 3). Sertoli cells were partially detached from the basement membrane (BM) of the seminiferous epithelium (Fig. 3, asterisks), and cell membranes of adjacent Sertoli cells were not joined (Fig. 3, arrows). Figure 4 shows the basal aspects of the seminiferous epithelium in the EI-300 testes. Although relatively normal spermatogonia and spermatocytes were observed in the seminiferous epithelium in EI-300 testes, Sertoli cells were shrunken, condensed and fully detached from the BM of the seminiferous epithelium (Fig. 4A). The BM of the seminiferous epithelium was normal and maintained its continuity (Fig. 4B, arrows), and the myoid cells were also relatively normal (Fig. 4B, M).

To examine the integrity of the BTB in EI testes, a lanthanum tracer study was performed. Figure 5A shows the basal aspect of the

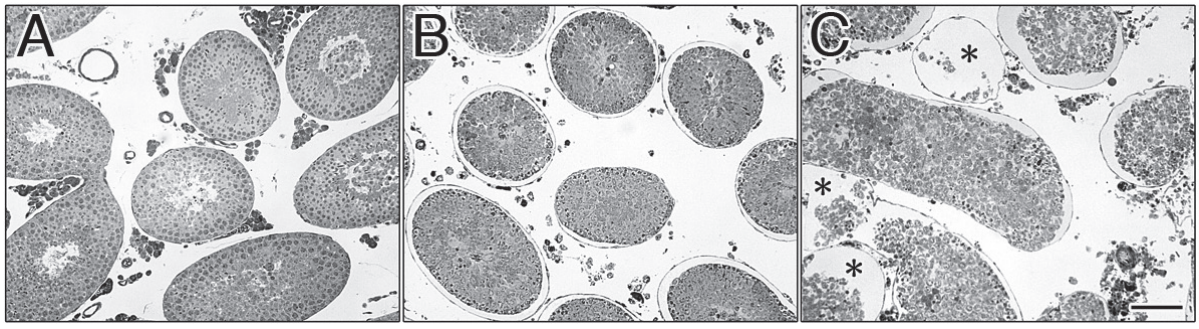

Fig. 1. Semithin sections of the EI testes. At 0 min (A; control sample), at 240 min (B) and at 300 min (C) after the EI procedure. Normal spermatogenesis was observed in the control (A). In EI-240 testes, the seminiferous epithelium was partially detached from the testicular lamina propria (B). The seminiferous epithelium was eliminated from the seminiferous tubules in EI-300 testes (C, asterisks). Scale bar, 100 μm.

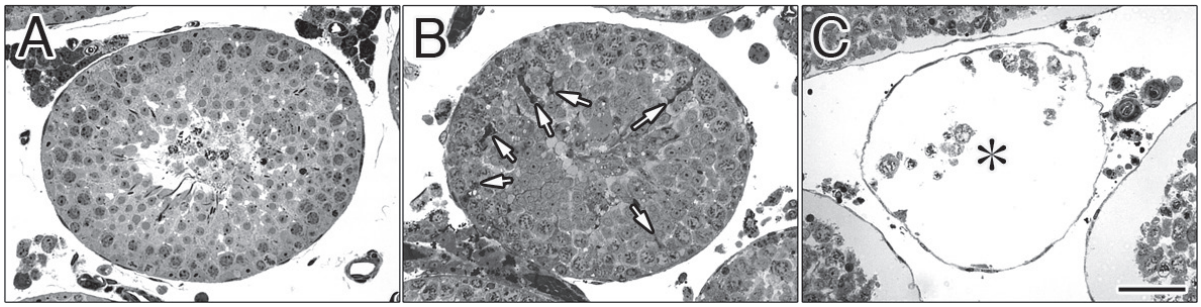

Fig. 2. Semithin sections of the seminiferous tubules in EI testes. At 0 min (A; control sample), at 180 min (B), and at 300 min (C) after the EI procedure. Normal spermatogenesis was observed in the control (A) and EI-180 testes (B). The white arrows in B indicate the regions densely stained with TB in the seminiferous epithelium. No evidence of spermatogenesis was observed in the seminiferous tubules in EI-300 testes (C, asterisk). Scale bar, 50 μm.

seminiferous epithelium of EI-240 testes. The tracer was not detected in the intercellular cleft around the germ cells (Fig. 5A). However, the tracer penetrated into the spaces between adjacent Sertoli cells in the adluminal compartment up to the lumen of the seminiferous tubules (Fig. 5B, arrows).

2D mapping of EI and control testes

To identify biochemical alterations caused by ischemia in the testicular tissues, we compared 2D maps of testis proteins extracted from control samples (right testes) and EI-180 testes. Figure 6 shows the 2D electrophoretic maps of the testis proteins extracted from the control testes (Fig. 6A) and EI-180 testes (Fig. 6B) respectively. Many of the protein spots were found in both maps, and the common spots are indicated by circles and numbered (Figs. 6A and B). The intensities of protein spots 5, 9, 10, 13, 18, 19 and 20 were significantly increased in EI-180 testes in comparison with the controls. The most significant upregulation was observed in spot 19 (Fig. 6B, arrow). This spot was excised, digested with V8 protease and sequenced. The internal amino acid sequence of spot 19 (I-V-L-V-G-G-S-T-R-I-P-K-I-Q-K-L-L-Q-D-F) was compared with known sequences using FASTA. The analysis demonstrated that spot 19 found in EI-180 testes was identical to mouse HSP72 (Accession Number: P17156; UniProt/Swiss-Prot).

SDS-PAGE and Western blot analysis of EI and control testes

Figure 7A shows the results of 12% SDS-PAGE; the proteins were stained with CBB or transferred to NC membranes and incubated with an anti-mouse HSP70 antibody. Western blotting analysis showed a single band (about 70 kDa) for all testes, but different intensities of HSP70 were found at different time points.

For a more objective and quantitative evaluation of these results, the intensity of HSP70 in Fig. 7A was quantitatively expressed, and each numerical value was graphed in Fig. 7B. The expression of HSP70 was time dependent from the beginning of EI until its peak at 180 min, after which it gradually decreased. The relative expression of HSP70 in EI-180 testes was significantly higher than that in other samples. It was upregulated approximately twofold at 120 min and over fourfold at 180 min after EI (Fig. 6B, $P < 0.05$).

Immunocytochemical microscopy with an anti-HSP70 antibody

In the negative control testes, the primary antibody was omitted, and no labeling was observed in germ cells. However, nonspecific staining of interstitial Leydig cells was visible around the seminiferous tubules (Fig. 8A). In the control testes, positive labeling of HSP70 was observed in a few spermatocytes (Fig. 8B, arrows). After the EI procedure, immunoperoxidase staining was observed in all round and elongated spermatids and spermatocytes (Figs. 8C and D).

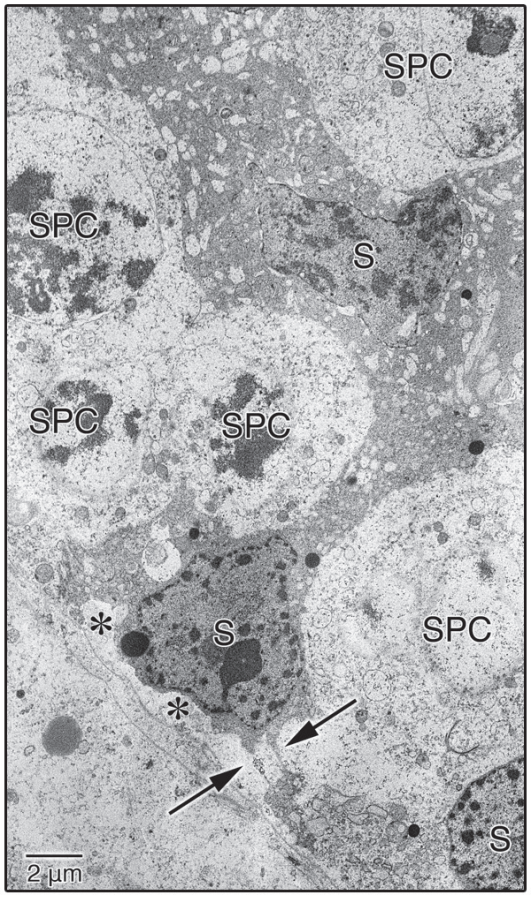

Fig. 3. TEM image of the seminiferous epithelium in EI-240 testes. Sertoli cells were partially detached from the BM of the seminiferous epithelium (asterisks), and the cell membranes of adjacent Sertoli cells were not joined (arrows). S, Sertoli cell; SPC, spermatocyte.

Discussion

The testes and adnexa of most scrotum-bearing mammals receive their vasculature from two sources: the internal spermatic artery, which arises from the aorta, and the deferential artery, which originates from the internal iliac or hypogastrium. One of the most startling aspects of the testicular vasculature is the gross anatomic configuration of the internal spermatic artery, the major source of blood supply. The internal spermatic artery continues as the testicular artery, supplying the testis. The superior epididymal branch of the testicular artery descends to the corpus epididymis, where it forms a well-defined anastomotic loop with the second source of blood supply, the deferential artery [8]. In this study, we induced EI in 35-day-old ICR male mice by clamping the testicular artery and vein. Because the deferential artery was intact in our model mice, necrosis did not develop. The purpose of this experimental system was to examine morphological changes immediately after clamping and to investigate the biochemical events taking place immediately before the morphological changes.

Our proteome analysis showed that mouse HSP72 was most significantly upregulated in EI-180 testes (Fig. 6B, arrow). HSP70 is one of the most highly conserved members of the HSP family and is constitutively expressed in the testis [14–17]. The inducible HSP72 isoform of HSP70 is expressed in heat-treated mouse testes [18, 19]. Because cells exposed to elevated temperatures respond by synthesizing HSPs, it is reasonable to assume that the rapid upregulation of HSP72 in EI testes was caused by heat stress induced by ischemia.

We also examined the expression and distribution pattern of HSP72 in EI testes using the anti-HSP70 polyclonal antibody, which recognizes the heat-induced HSP72. Western blotting revealed a faint signal with a single band at approximately 70 kDa in the control testes (Fig. 7A). Immunohistochemical microscopy using the same antibody for the control testes showed positive signals in a few

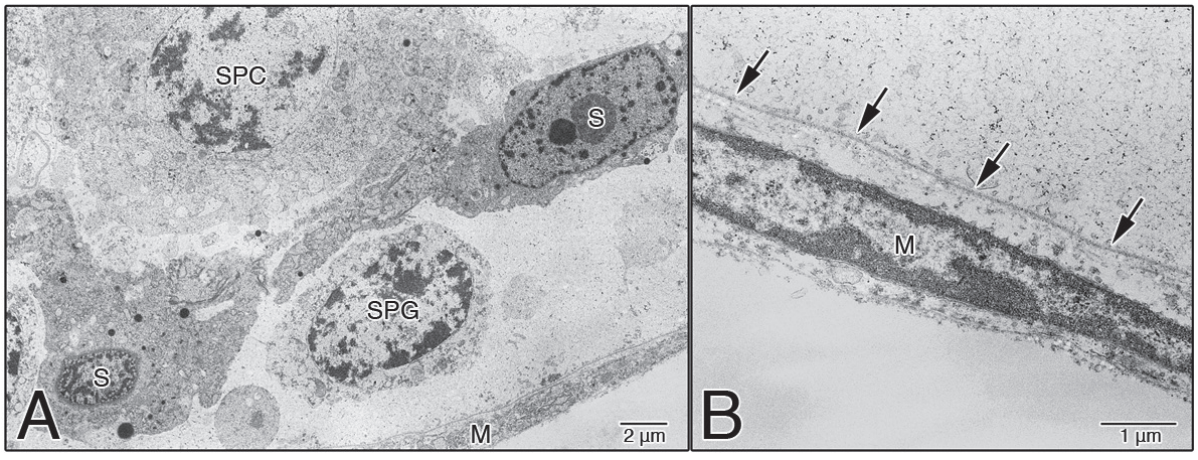

Fig. 4. Basal aspects of the seminiferous epithelium in EI-300 testes. Sertoli cells were shrunken, condensed, and fully detached from the BM of the seminiferous epithelium, but relatively normal spermatogonia and spermatocytes were observed (A). The BM of the seminiferous epithelium was relatively normal and maintained its continuity (arrows in B), and the myoid cells were also relatively normal (B). S, Sertoli cell; SPG, spermatogonium; SPC, spermatocyte; M, myoid cell.

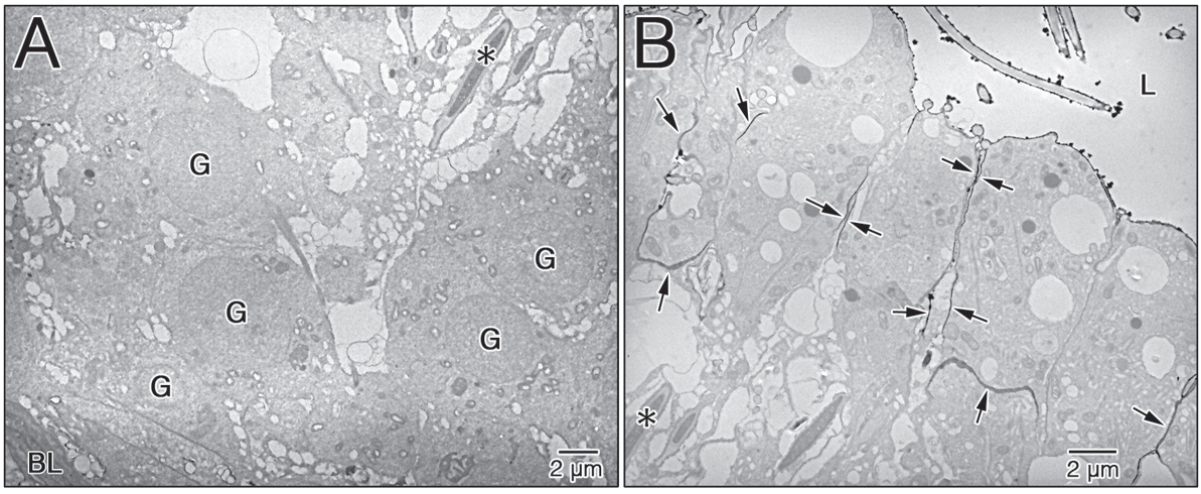

Fig. 5. Integrity of the BTB in EI testes. The seminiferous epithelium of EI-240 testes after the administration of lanthanum; thin sections were examined without staining. The tracer was not detected in the intercellular cleft around the germ cells (A). In contrast, the electron tracer penetrated into the spaces between adjacent Sertoli cells in the adluminal compartment up to the lumen (B, arrows). The asterisk indicates the same mature spermatid (A and B). L, lumen of seminiferous tubule; G, germ cell; BL, basal lamina.

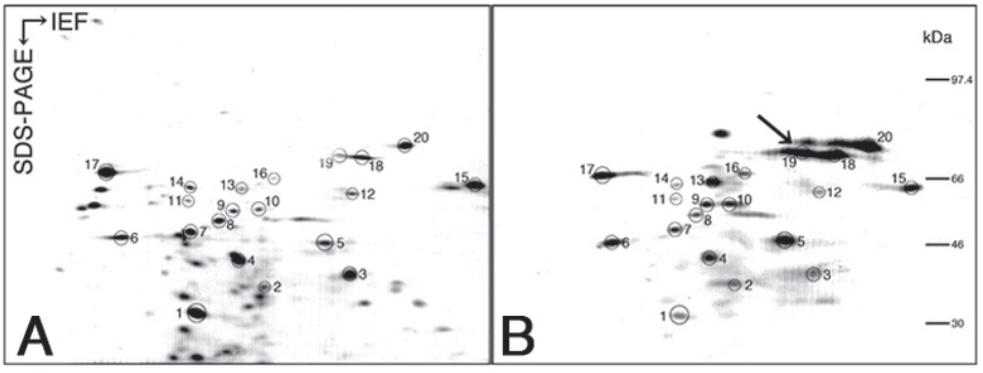

C

```
1 MSARGPAIGI DLGTTYSCVG VFQHGKVEII ANDQGNRTTP SYVAFTDTER LIGDAAKNQV
61 AMNPTNTIFD AKRLIGRKFE DATVQSDMKH WPFRVVSEGG KPKVQVEYKG EMKTFFPEEI
121 SSMVLTKMKE IAEAYLGGKV QSAVITVPAY FNDSQRQATK DAGTITGLNV LRIINEPTAA
181 AIAYGLDKKG CAGGEKNVLI FDLGGGTFDV SILTIEDGIF EVKSTAGDTH LGGEDFDNRM
241 VSHLAEEFKR KHKKDIGPNK RAVRRLRTAC ERAKRTLSSS TQASIEIDSL YEGVDFYTSI
301 TRARFEELNA DLFRGTLEPV EKALRDAKLD KGQIQEIVLV GGSTRIPKIQ KLLQDFFNGK
361 ELNKSINPDE AVAYGAAVQA AILIGDKSEN VQDLLLLDVT PLSLGIETAG GVMTPLIKRN
421 TTIPTKQTQT FTTYSDNQSS VLVQVYEGER AMTKDNNLLG KFDLTGIPPA PRGVPQIEVT
481 FDIDANGILN VTAADKSTGK ENKITITNDK GRLSKDDIDR MVQEAERYKS EDEANRDRVA
541 AKNAVESYTY NIKQTVEDEK LRGKISEQDK NKILDKCQEV INWLDRNQMA EKDEYEHKQK
601 ELERVCNPII SKLYQGGPGG GGSSGGPTIE EVD
```

Fig. 6. Proteome analysis of the EI testes. Two-dimensional mapping of testis proteins in the control (A) and EI-180 testes (B). Full-length amino acid sequence of mouse HSP72 (C). Spots expressed in both testes are indicated by circles and are numbered. The most significant upregulation was observed in spot 19 (B, arrow). The matching amino acid residues are highlighted in black (C).

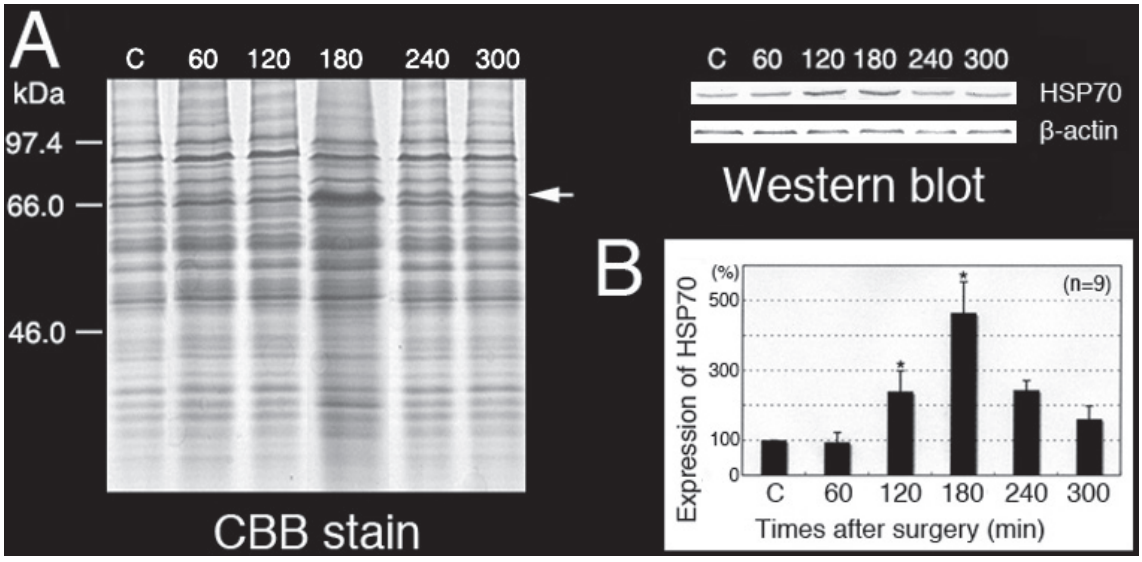

Fig. 7. Expression of HSP70 in the EI testes. SDS-PAGE and Western blot analysis of the control testes and testes at different times after the EI procedure. The anti-HSP70 polyclonal antibody reacted with a single band at approximately 70 kDa (A, arrow). Relative intensity of HSP70 in the control testes and testes at different times after the EI procedure (B). * $P < 0.05$. Values are shown as the mean ± SE.

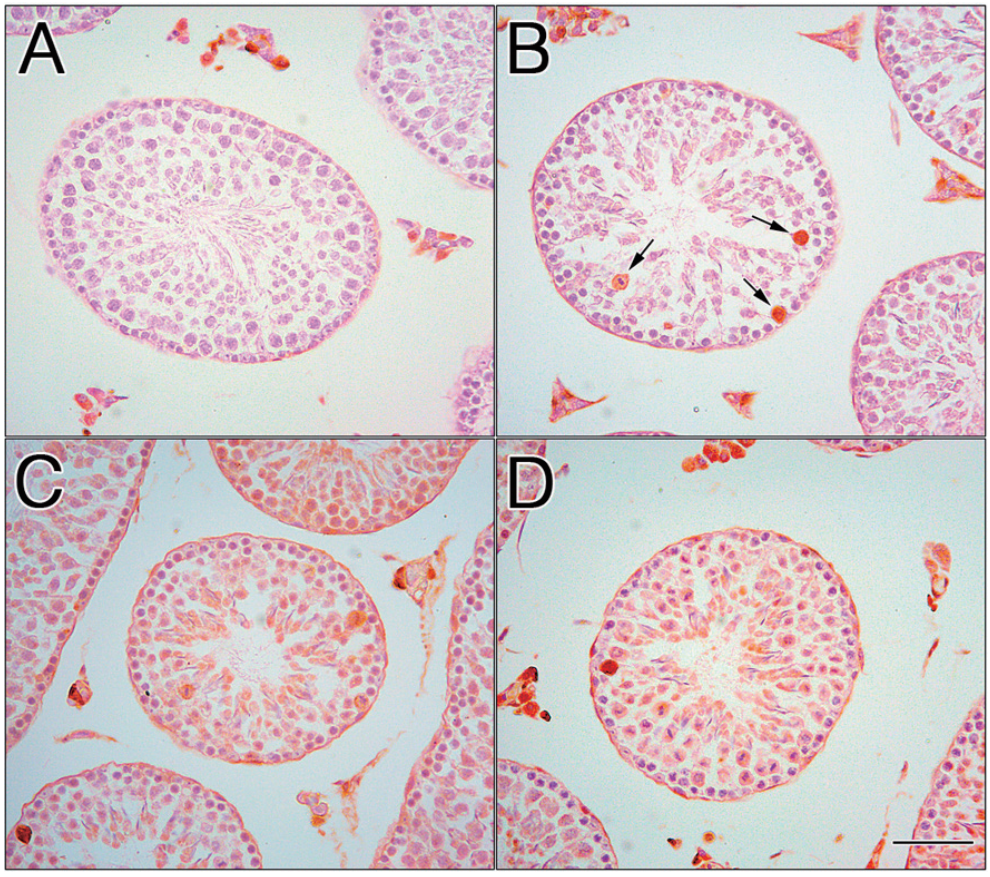

Fig. 8. Localization of HSP70 in the EI testes. In the negative control testis, the primary antibody was omitted, and no labeling of germ cells was observed. Nonspecific staining of Leydig cells was observed in interstitial tissues (A). In the control testis, positive labeling was observed in a few spermatocytes (B, arrows). In EI-120 (C) and EI-180 (D) testes, immunoperoxidase staining was also observed in all round and elongated spermatids and spermatocytes. Scale bar, 50 μm.

spermatocytes (Fig. 8B). A unique pattern of HSP70 expression is associated with mouse spermatogenesis. Spermatocyte-specific HSP70, called HSP70-2, is expressed in pachytene spermatocytes during the meiotic phase [20–25]. The amino acid sequences of HSP70-2 are highly similar to those of heat-inducible HSP70s. HSP72 is a minor protein not usually detected in unstressed rodent cells [18]; the faint signal detected by Western blotting in the control testes (Fig. 7A) may correspond to the spermatocyte-specific immunoperoxidase staining shown in Figure 8B. Our results suggest that this faint signal in the control testes is a cross-reaction of the HSP70 polyclonal antibody with HSP70-2.

The Western blot analysis revealed that HSP72 was overexpressed approximately twofold at 120 min and over fourfold at 180 min after the EI procedure (Fig. 7B). In control samples, immunoperoxidase staining was localized in a few spermatocytes (Fig. 8B). After the EI procedure, increased immunoperoxidase staining was observed in both spermatocytes and round and elongated spermatids (Figs. 8C and D). These observations are in agreement with those of studies reporting that spermatocytes and round spermatids are the most heat-susceptible germ cells [26, 27]. The upregulation of HSP72 after the EI procedure, as observed by Western blotting, was correlated with HSP72 localization in spermatocytes and round and elongated spermatids, as observed by immunoperoxidase staining (Figs. 8C and D). Until 240 min after EI, EI caused morphological damage in Sertoli cells, but relatively normal germ cells were observed in the seminiferous epithelium (Figs. 1–4). This relatively low level of damage in both spermatocytes and round and elongated spermatids may be explained by the fact that HSP72 inhibits the release of mitochondrial apoptosis-inducing factor [17–19]. The expression of HSP72 was time dependent from the beginning of EI until its peak at 180 min, after which it gradually decreased. This decline in HSP72 expression 180 min after the EI procedure was correlated with the degree of degenerating seminiferous tubules (Figs. 1 and 2).

The existence of a functional barrier between the blood and lymph systems and the interior of the seminiferous tubules is well established [28]. This barrier maintains germ cells in an immunologically privileged location. The integrity of the BTB is a prerequisite for normal spermatogenesis. Using light microscopy, we demonstrated that, under EI, the initial morphological damage occurred in EI-180 Sertoli cells (Fig. 2B). No morphological or size differences were detected in the seminiferous tubules among the control, EI-60 and EI-120 testes (data not shown). The TEM examination revealed that EI-240 Sertoli cells were partially detached from the BM of the seminiferous epithelium (Fig. 3, asterisks) and that the cell membranes of adjacent Sertoli cells were not joined (Fig. 3, arrows). To examine the integrity of the BTB in EI-240 testes, a lanthanum tracer study was performed. In EI-240 testes, the electron tracer penetrated into the spaces between adjacent Sertoli cells in the adluminal compartment up to the lumen (Fig. 5B, arrows). This result suggests that a change in the junctions between adjacent Sertoli cells on the basal compartment is involved in the BTB disruption in EI testes. Therefore, male infertility caused by the BTB disruption could be associated with heat stress induced by ischemia. There was no evidence of spermatogenesis in EI-300 seminiferous tubules (Fig. 2C). However, the BTB does not change morphologically, and the integrity of the BTB is not affected in experimental cryptorchidism [29, 30]. There are no haploid germ cells in the seminiferous epithelium in mice 14 days after cryptorchid surgery [30]. These facts suggest that the loss of haploid germ cells in heat shock may inhibit the differentiation into haploid germ cells from diploid germ cells by an endogenous factor of the testis. In male germ cells, high temperatures induce an increase in the synthesis of several proteins and a decrease in many others [31–34]. Changes in the distribution pattern of ZO-1 have been related to an increased permeability of tight junctions by a number of previous studies. Fink *et al*. noted weak and diffuse staining for ZO-1 and ZO-2 in the BTB region within carcinoma *in situ* tubules [35]. The disruption of the BTB may be related to the dislocation of ZO-1 and ZO-2 to the Sertoli cell cytoplasm. Further research is warranted to explain the detailed mechanisms maintaining the functional integrity of the BTB.

References

1. **Iammarrone E, Balet R, Lower AM, Gillott C, Grudzinskas JG.** Male infertility. *Best Pract Res Clin Obstet Gynaecol* 2003; **17**: 211–229.
2. **Smith JF, Eisenberg ML, Millstein SG, Nachtigall RD, Shindel AW, Wing H, Cedars M, Pasch L, Katz PP, Infertility Outcomes Program Project Group.** The use of complementary and alternative fertility treatment in couples seeking fertility care: data from a prospective cohort in the United States. *Fertil Steril* 2010; **93**: 2169–2174.
3. **Krausz C.** Male infertility: pathogenesis and clinical diagnosis. *Best Pract Res Clin Endocrinol Metab* 2011; **25**: 271–285.
4. **Jungwirth A, Giwercman A, Tournaye H, Diemer T, Kopa Z, Dohle G, Krausz C, European Association of Urology Working Group on Male Infertility.** European association of urology guidelines on male infertility: the 2012 update. *Eur Urol* 2012; **62**: 324–332.
5. **McLachlan JA, Newbold RR, Burow ME, Li SF.** From malformations to molecular mechanisms in the male: three decades of research on endocrine disrupters. *APMIS* 2001; **109**: 263–272.
6. **Itoh N, Kayama F, Tatsuki TJ, Tsukamoto T.** Have sperm counts deteriorated over the past 20 years in healthy, young Japanese men? Results from the Sapporo area. *J Androl* 2001; **22**: 40–44.
7. **Deng Y, Zhang W, Su D, Yang Y, Ma Y, Zhang H, Zhang S.** Some single nucleotide polymorphisms of MSY2 gene might contribute to susceptibility to spermatogenic impairment in idiopathic infertile men. *Urology* 2008; **71**: 878–882.
8. **Gunn SA, Gould TC.** Vasculature of the testes and adnexa. *In*: Hamilton DW, Greep RO (eds.), Handbook of Physiology. American Physiological Society, Washington DC; 1975: 117–142.
9. **McLean IW, Nakane PK.** Periodate-lysine-paraformaldehyde fixative. A new fixation for immunoelectron microscopy. *J Histochem Cytochem* 1974; **22**: 1077–1083.
10. **O'Farrell PH.** High resolution two-dimensional electrophoresis of proteins. *J Biol Chem* 1975; **250**: 4007–4021.
11. **Hirano H.** Varietal differences of leaf protein profiles in mulberry. *Phytochemistry* 1982; **21**: 1513–1518.
12. **Cleveland DW, Fischer SG, Kirschner MW, Laemmli UK.** Peptide mapping by limited proteolysis in sodium dodecyl sulfate and analysis by gel electrophoresis. *J Biol Chem* 1977; **252**: 1102–1106.
13. **Hirano H. W-Liebold B.** Protein microsequence analysis with dansyl-amino-PITC. *In*: W-Liebold B (ed.), Methods in Protein Sequence Analysis. Springer, Berlin; 1989: 42–51.
14. **Allen RL, O'Brien DA, Eddy EM.** A novel hsp70-like protein (P70) is present in mouse spermatogenic cells. *Mol Cell Biol* 1988; **8**: 828–832.
15. **Allen RL, O'Brien DA, Jones CC, Rockett DL, Eddy EM.** Expression of heat shock proteins by isolated mouse spermatogenic cells. *Mol Cell Biol* 1988; **8**: 3260–3266.
16. **Rosario MO, Perkins SL, O'Brien DA, Allen RL, Eddy EM.** Identification of the gene for the developmentally expressed 70 kDa heat-shock protein (P70) of mouse spermatogenic cells. *Dev Biol* 1992; **150**: 1–11.
17. **Zakeri ZF, Welch WJ, Wolgemuth DJ.** Characterization and inducibility of hsp 70 proteins in the male mouse germ line. *J Cell Biol* 1990; **111**: 1785–1792.
18. **Ellis S, Killender M, Anderson RL.** Heat-induced alterations in the localization of HSP72 and HSP73 as measured by indirect immunohistochemistry and immunogold electron microscopy. *J Histochem Cytochem* 2000; **48**: 321–332.
19. **Zaprjanova S, Rashev P, Zasheva D, Martinova Y, Mollova M.** Electrophoretic and immunocytochemical analysis of Hsp72 and Hsp73 expression in heat-stressed mouse testis and epididymis. *Eur J Obstet Gynecol Reprod Biol* 2013; **168**: 54–59.

20. **Dix DJ, Allen JW, Collins BW, Mori C, Nakamura N, Poorman-Allen P, Goulding EH, Eddy EM.** Targeted gene disruption of Hsp70-2 results in failed meiosis, germ cell apoptosis, and male infertility. *Proc Natl Acad Sci USA* 1996; **93**: 3264–3268.
21. **Zhou XC, Han XB, Hu ZY, Zhou RJ, Liu YX.** Expression of Hsp70-2 in unilateral cryptorchid testis of rhesus monkey during germ cell apoptosis. *Endocrine* 2001; **16**: 89–95.
22. **Mori C, Nakamura N, Dix DJ, Fujioka M, Nakagawa S, Shiota K, Eddy EM.** Morphological analysis of germ cell apoptosis during postnatal testis development in normal and Hsp 70-2 knockout mice. *Dev Dyn* 1997; **208**: 125–136.
23. **Vydra N, Malusecka E, Jarzab M, Lisowska K, Glowala-Kosinska M, Benedyk K, Widlak P, Krawczyk Z, Widlak W.** Spermatocyte-specific expression of constitutively active heat shock factor 1 induces HSP70i-resistant apoptosis in male germ cells. *Cell Death Differ* 2006; **13**: 212–222.
24. **Yazama F, Furuta K, Fujimoto M, Sonoda T, Shigetomi H, Horiuchi T, Yamada M, Nagao N, Maeda N.** Abnormal spermatogenesis in mice unable to synthesize ascorbic acid. *Anat Sci Int* 2006; **81**: 115–125.
25. **Sasaki T, Marcon E, McQuire T, Arai Y, Moens PB, Okada H.** Bat3 deficiency accelerates the degradation of Hsp70-2/HspA2 during spermatogenesis. *J Cell Biol* 2008; **182**: 449–458.
26. **Kaushal N, Bansal MP.** Selenium variation induced oxidative stress regulates p53 dependent germ cell apoptosis: plausible involvement of HSP70-2. *Eur J Nutr* 2009; **48**: 221–227.
27. **Ruchalski K, Mao H, Singh SK, Wang Y, Mosser DD, Li F, Schwartz JH, Borkan SC.** HSP72 inhibits apoptosis-inducing factor release in ATP-depleted renal epithelial cells. *Am J Physiol Cell Physiol* 2003; **285**: C1483–C1493.
28. **Setchell BP, Waites GMH.** The blood-testis barrier. *In*: Hamilton DW, Greep RO (eds.), Handbook of Physiology. American Physiological Society, Washington DC; 1975: 143–172.
29. **Hagenäs L, Plöen L, Ritzen EM, Ekwall H.** Blood-testis barrier: maintained function of inter-Sertoli cell junctions in experimental cryptorchidism in the rat, as judged by a simple lanthanum-immersion technique. *Andrologia* 1977; **9**: 250–254.
30. **Yazama F.** Continual maintenance of the blood-testis barrier during spermatogenesis: the intermediate compartment theory revisited. *J Reprod Dev* 2008; **54**: 299–305.
31. **Biggiogera M, Tanguay RM, Marin R, Wu Y, Martin TE, Fakan S.** Localization of heat shock proteins in mouse male germ cells: an immunoelectron microscopical study. *Exp Cell Res* 1996; **229**: 77–85.
32. **Cataldo L, Mastrangelo MA, Kleene KC.** Differential effects of heat shock on translation of normal mRNAs in primary spermatocytes, elongated spermatids, and Sertoli cells in seminiferous tubule culture. *Exp Cell Res* 1997; **231**: 206–213.
33. **Dix DJ.** Hsp70 expression and function during gametogenesis. *Cell Stress Chaperones* 1997; **2**: 73–77.
34. **Fujisawa M, Matsumoto O, Kamidono S, Hirose F, Kojima K, Yoshida S.** Changes of enzymes involved in DNA synthesis in the testes of cryptorchid rats. *J Reprod Fertil* 1988; **84**: 123–130.
35. **Fink C, Weigel R, Hembes T, Lauke-Wettwer H, Kliesch S, Bergmann M, Brehm RH.** Altered expression of ZO-1 and ZO-2 in Sertoli cells and loss of blood-testis barrier integrity in testicular carcinoma *in situ*. *Neoplasia* 2006; **8**: 1019–1027.